Section S1. Materials and reagents

All reagents were at least ACS reagent grade or higher and were used without any further purification. 4-nitrophenol (≥99%), hydroquinone (≥99.5%), 4-nitrocatechol (≥97%), 1,2,4-trihydroxybenzene (≥99%), 2-nitrophloroglucinol (95%), phloroglucinol (≥99.5%), hydrogen peroxide solution in water (≥30% ultratrace, no stabilizers added), acetic anhydride (≥99%), sodium chloride (≥99%), sodium phosphate dibasic (≥99%), HPLC-grade solvents: ethyl acetate (≥99.5%), methanol (≥99.9%) as well as the plastic UV-Vis cuvettes (P/N Z637157) with 1 cm absorption pathlength and the effective wavelength range 230-900 nm were all purchased from Sigma Aldrich (Schnelldorf, Germany). Anhydrous sodium sulfate (fine powder, ≥99%), sodium hydroxide (≥99%), hydrochloric acid (35-37% solution in water) were obtained from Avantor Performance Materials (Gliwice, Poland). Perchloric acid (65% solution in water) was obtained from Chempur (Piekary Śląskie, Poland). Deionized (DI) water (18 MΩ × cm^{-1}) was prepared using Direct - Q3 Ultrapure Water System (Millipore). Ultra-high purity (UHP) helium (GC/MS carrier gas) and UHP oxygen (used in the total organic carbon analyzer) were supplier by Multax (Stare Babice, Poland).

Section S2. Dissociation of 4-nitrophenol as a function of pH

The pKa value of 4-nitrophenol was previously reported as ca. 7.15 (Zhao et al., 2015; Vione et al., 2009) and it was used to evaluate the concentration ratio of protonated and deprotonated forms of this compound under the experimental conditions used.

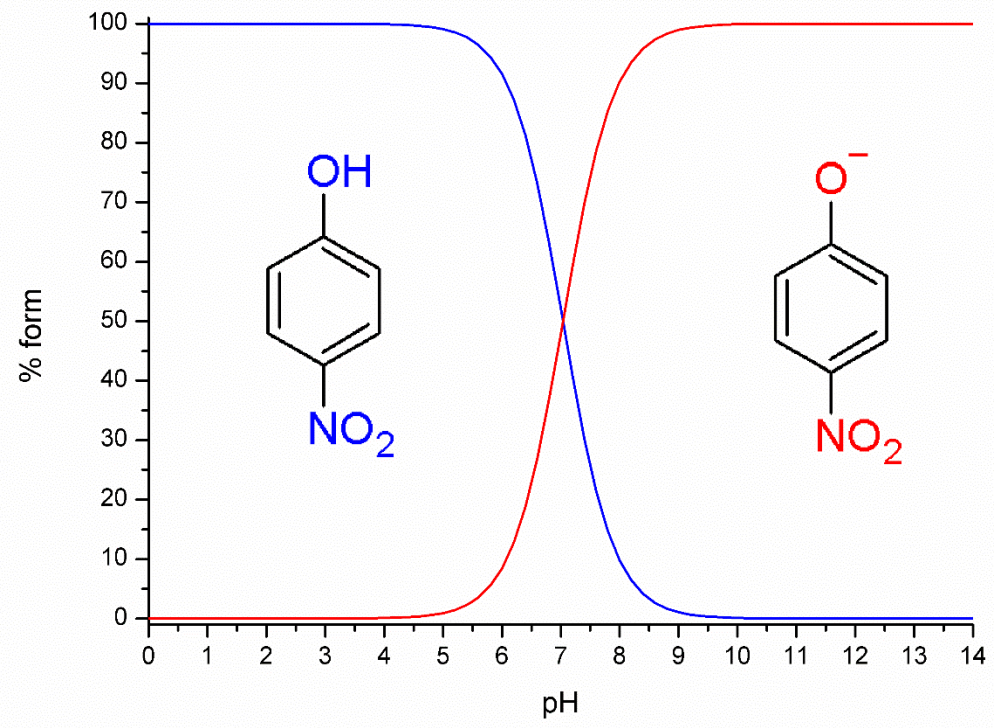

Figure S1: Dissociation curve of 4-nitrophenol as a function of pH.

As presented in Fig. S1, at pH=2 or pH=9, 4-nitrophenol was present in the aqueous solution as completely protonated or as nitrophenolate ion, respectively. Hence, under the experimental conditions used it was possible to investigate the OH reaction with completely protonated and deprotonated 4-nitrophenol

Section S3. Steady-state concentration of hydroxyl radicals in the absence of organic reactants

The concentration of OH in the absence of organic reactants was estimated by monitoring the disappearance of H_2O_2 in DI water following photolysis in the photoreactor at 298 K (section S2.1). The first-order rate of photolysis was then estimated with a kinetic box-model (Tan et al., 2009) – results are presented in Fig. S2.

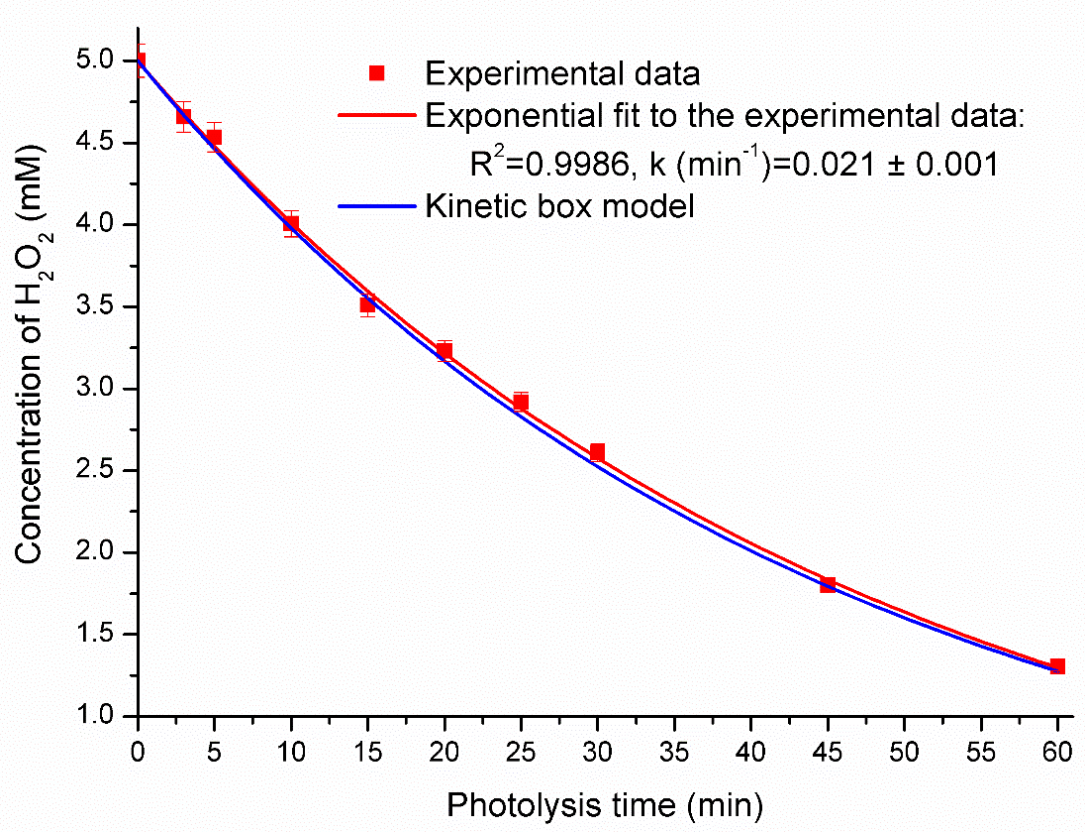

Figure S2: Photolysis of H2O2 in the photochemical reactor.

As presented in Fig. S2, the kinetic box model accurately reproduced the photolysis of H_2O_2 resulting in a first-order photolysis rate of 1.9×10^{-4} s^{-1}. The estimated steady-state concentration of OH in the absence of organic reactants was 1.4×10^{-9} M. This value is much higher than the upper limit of OH concentration in cloud water but allowed for simulating the aqueous chemical processing of 4-nitrophenol via OH within a reasonable time-scale.

Section S4. Experimental details

Section S4.1. Photooxidation of 4-nitrophenol in the aqueous photoreactor

The photooxidation reaction was carried out in a custom-made quartz, jacketed reaction vessel with the internal volume of 100 ml. The reaction vessel was closed with a glass stopper and placed inside the photochemical reactor that is described in more detail elsewhere (Witkowski et al., 2019).

The reaction mixture consisted of the deionized water and 4-nitrophenol (concentration between 100 and 350 μM) and the pH was adjusted to 2 or 9 using HCl, $HClO_4$ or Na_2HPO_4. The pH was checked with the HI 221 pH-meter (Hanna Instruments) before and after each experiment. The pH meter was calibrated daily with pH=4.01, 7.00 and 10.00 buffer solutions. After adjusting the pH, the reaction solution was filtered through 1.2 μm glass microfiber syringe filter and transferred into the reaction vessel. The zero-time sample was withdrawn from the reactor and then H_2O_2 was added (initial concentration of H_2O_2 in the reaction mixture was 5 mM - Fig. S2). Aliquots of the reaction mixture were withdrawn periodically from the photoreactor at five minutes intervals and the total reaction time was 60 min.

Photoreactor used in this work was equipped with a circular set of eight 4W, G5-socket lamps. Out of all eight lamps in the photoreactor, two were UVC, mercury lamps with the peak emission 254 nm (TUV TL 4W, Philips). The UVC lamps were placed opposite to each other for a symmetric irradiation of the reaction mixture. The other six lamps were emitting visible light above 400nm. Such a mixed set of lamps was used to limit the amount of short-wavelength UVC irradiation in order to avoid direct photolysis of phenols under investigation (Table S1). At the same time, the amount of UVC irradiation was sufficient to efficiently produce OH via H_2O_2 photolysis. Hence, it was possible to investigate 4-nitrophenol reaction with the OH while avoiding direct photolysis of the reactants – see also section S4.2.

The reactor lamps were allowed to warm up on for at least 30 min prior starting of the experiment. The fan placed at the bottom of the photoreactor prevented the lamps from overheating by forcing the air flow thought the inside portion of the circular set of lamps. The stirring bar was placed inside the reaction vessel for the continuous stirring of the mixture with a bullied-in magnetic stirrer. The water was circulated in the outer jacket of the quartz reaction vessel to maintain the temperature of the reaction mixture at 298 K using a circulating bath (SC100 a10, Thermo Fisher Scientific).

Section S4.2. Analysis of phenols with GC/MS

The sample volume was 250µl; each sample of the reaction mixture was added to a 2.5 ml of the aqueous solution of Na_2HPO_4 (concentration 20 g/L, pH=7.4) and NaCl (concentration 28 g/L) in a 4 ml glass vial and immediately derivatized. 10 µl of phloroglucinol (internal standard) solution in DI water (concentration 0.5 g/L) was added followed by 20 µl of acetic anhydrite; the derivatization reaction was carried out for 1h. After 1h, each aqueous sample was extracted with 300 µl of ethyl acetate via mechanical agitation for ca. 20 s. The top organic layer was separated, dried with the anhydrous Na_2SO_4 via mechanical agitation and then centrifuged for 10 min in order to separate the solid residue from the organic layer. Organic layer was transferred into a separate vial with a 300 µl fused-in glass insert and 1µl of the dried ethyl acetate was injected into GC/MS. GC/MS analyses were carried out using GC-MS-QP2010 Ultra gas chromatograph (Shimadzu) interfaced with the single quadrupole QP-5000 mass spectrometer (Shimadzu). The instrument was equipped with AOC-5000 autosampler (Shimadzu) that was used in the liquid-injection mode and equipped with a 10 µl syringe. The syringe was washed five times before and after each injection, firstly with 8µl of methanol and subsequently with 8µl ethyl acetate. The purpose of this extensive washing of the syringe was to avoid accumulation of the solid Na_2SO_4 that caused clogging of the syringe needle and prevented the plunger from moving smoothly as inferred from the initial experiments.

The analytes were separated using capillary column ZB-5MSPlus (Phenomenex): 30m x 0.25mm, 0.25 µm of the stationary phase. The column head pressure was 26.7 kPa, the total flow of the carried gas was 10.5 ml/min, column flow 0.68 ml/min (30 cm/sec), purge flow was 3 ml/min. The linear velocity flow control mode was used and the split ratio was 10. The temperatures of injector, ion source and the mass spectrometer were 280°C. The following temperature program was used: initially 50 °C held for 5 min, then linear increase at the rate of 14 °C/min to 280°C, kept for 7 min, the total analysis time was 28 min. Electron impact ionization (EI) was used to ionize the analytes eluting from the capillary column and the mass spectrometer was operating in the selected ion monitoring mode (SIM) – see Table S1 - and the solvent cut was 6 min. GCMS solution 2.53 (Shimadzu) program was used for data acquisition and processing. Standards, m/z of the ions selected for the SIM mode and the tested linearity range of the MS detector under the experimental conditions used are listed in Table S1.

Table S1. List of standards and the parameters of the GC/MS analysis method

Name	**Ions monitored in SIM mode (m/z)**	**Retention time (min)**	**Concentration range (g/L)**	**Squared linear coefficient of determination (R^2)**
Hydroquinone	43, 110, 152	14.8	0.0025-0.038	0.9993
4-nitrophenol	43, 65, 81, 93, 123, 139, 181	15.1	0.0025-0.037	0.9977
1,2,4-Trihydroxybenzene	43, 126, 168, 210	17.3	0.0025-0.037	0.9949
4-Nitrocatechol	43, 81, 125, 139, 155, 181, 197	17.4	0.0025-0.037	0.9949
Phloroglucinol	*43, 126, 168, 210*	*17.6*	*0.023*	*Internal standard*
4-Nitrophloroglucinol	43, 125, 153, 171, 213, 255	18.9	0.0025-0.038	0.9981

As listed in Table S1, phloroglucinol was used as an internal standard for quantification of the phenols listed. 4-Nitrophloroglucinol was not produced via OH+4-nitrophenol reaction and was used as a surrogate standard for quantification of 4-nitropyrogallol and 5-nitropyrogallol that were both detected in the reaction mixture. Sample chromatogram of the standard mixture of phenols listed in Table S1 is shown in Fig. S3.

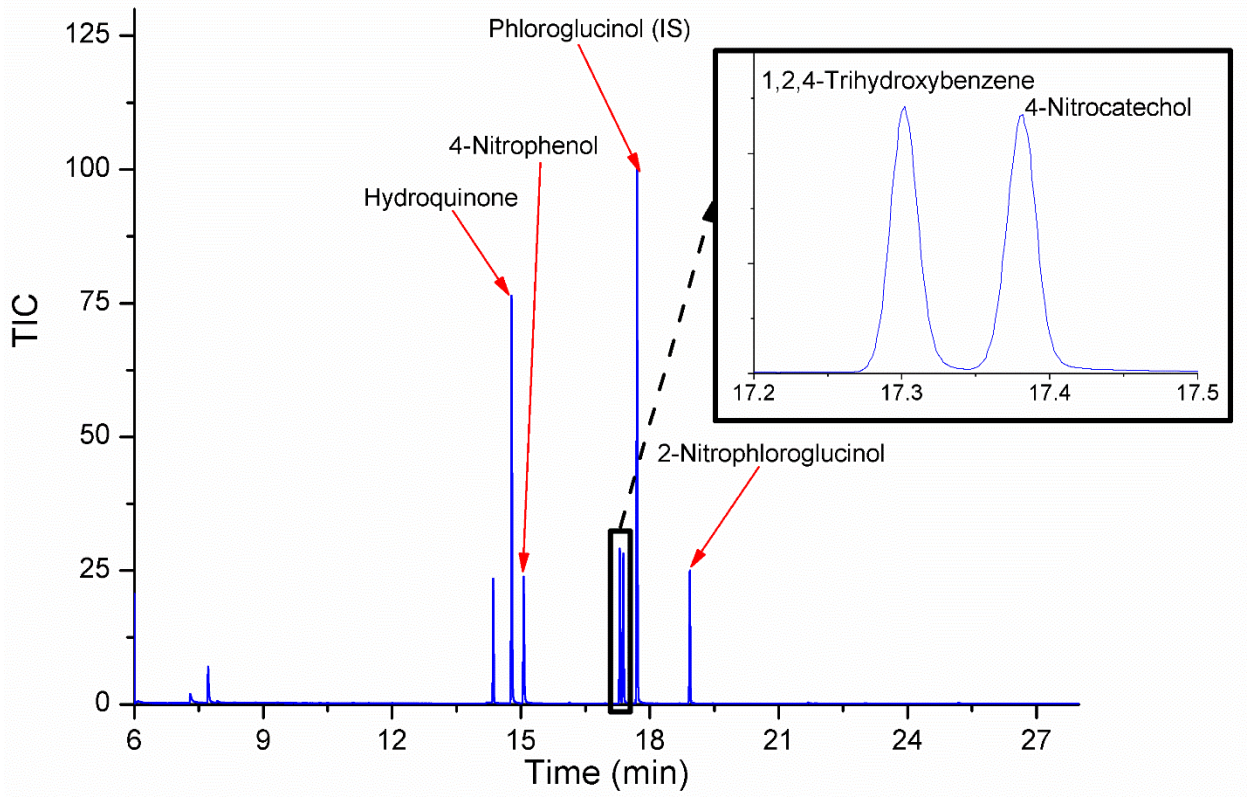

Figure S3: Chromatogram of the standard mixture of phenols listed in Table S1 detected as their acetyl derivatives.

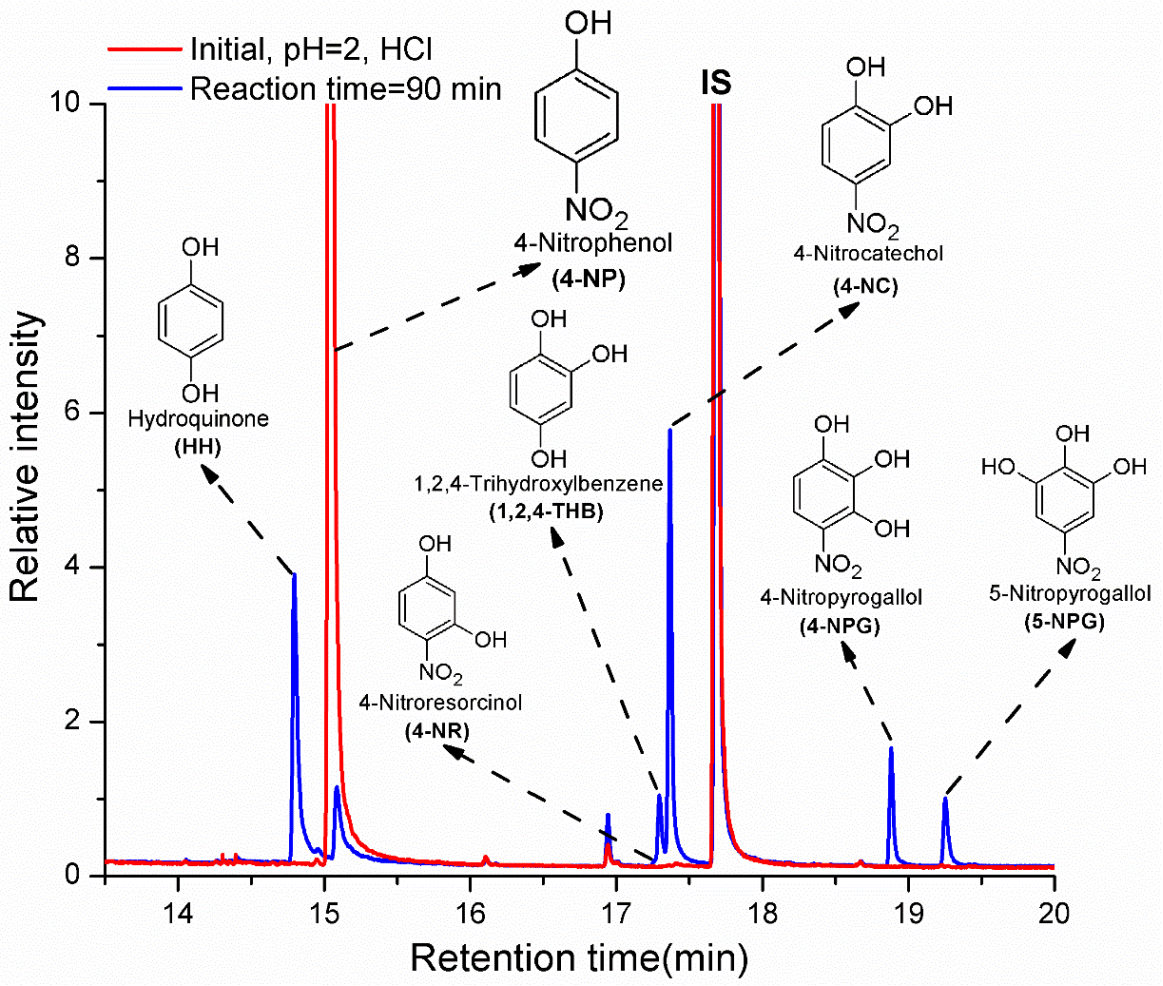

Figure S4: Chromatograms illustrating the formation of phenolic products from 4-NP oxidation by OH at pH=2.

95

Section S4.3. UV-Vis measurements

UV-Vis measurements were carried out with i8 dual-beam spectrometer (Envisense) in 4 ml cuvettes with a 1 cm absorption pathway using plastic cuvettes with wavelength range 230-900 nm. The wavelength-dependent cross sections, ε, ($mol^{-1}\times L\times cm^{-3}$) were measured for 4-nitrophenol, HH, HQL, 4-nitrocatechol and 2-NCG at a spectral resolution of 1 nm between 230 and 600 nm. For each phenol listed, ten standard solutions were prepared with concentrations between 1 and 6×10^{-5} M. The pH of standard solutions was between 2 – 9 (changed by 1 pH unit) and was adjusted with phosphoric acid or sodium hydroxide.

The absorbance of the 4-nitrophenol solution during the reaction with the OH (see sections 2.2 and S2.2) was measured between λ = 230 and 600 nm by periodically sampling 300 µl samples from the reaction mixture. Each 300 µl aliquot was then diluted with 2 ml of a buffer solution. After measuring the absorbance, the pH was adjusted by adding a small volume of NaOH or H_3PO_4 solution in DI water. A microelectrode was inserted directly into to the UV-Vis cuvettes to measure the pH of each sample before the absorbance was recorded. After adjusting the pH, the UV-Vis spectrum was recorded again and this procedure was repeated for each sample until pH=9 was reached. The absorbance measured for each sample was corrected for the dilution using the volume of the added buffering agent.

Section S5. UV-Vis absorption cross sections of 4-nitrophenol, hydroquinone, 4-nitrocatechol, 1,2,4-trihydroxybeneze and 2-nitrophloroglucinol

The UV-Vis absorption cross sections of 4-nitrophenol, hydroquinone, 4-nitrocatechol, 1,2,4-trihydroxybeneze and 2-nitrophloroglucinol were measured between pH 2 and 9 (section S2.3). Note that hydroquinone, 4-nitrocatechol, 1,2,4-trihydroxybeneze were unstable at pH>7, thus the ε values were not measured for these compounds at pH=8 and are not included in Fig. S5. The data presented in Fig. S5 is provided in appendix 1.

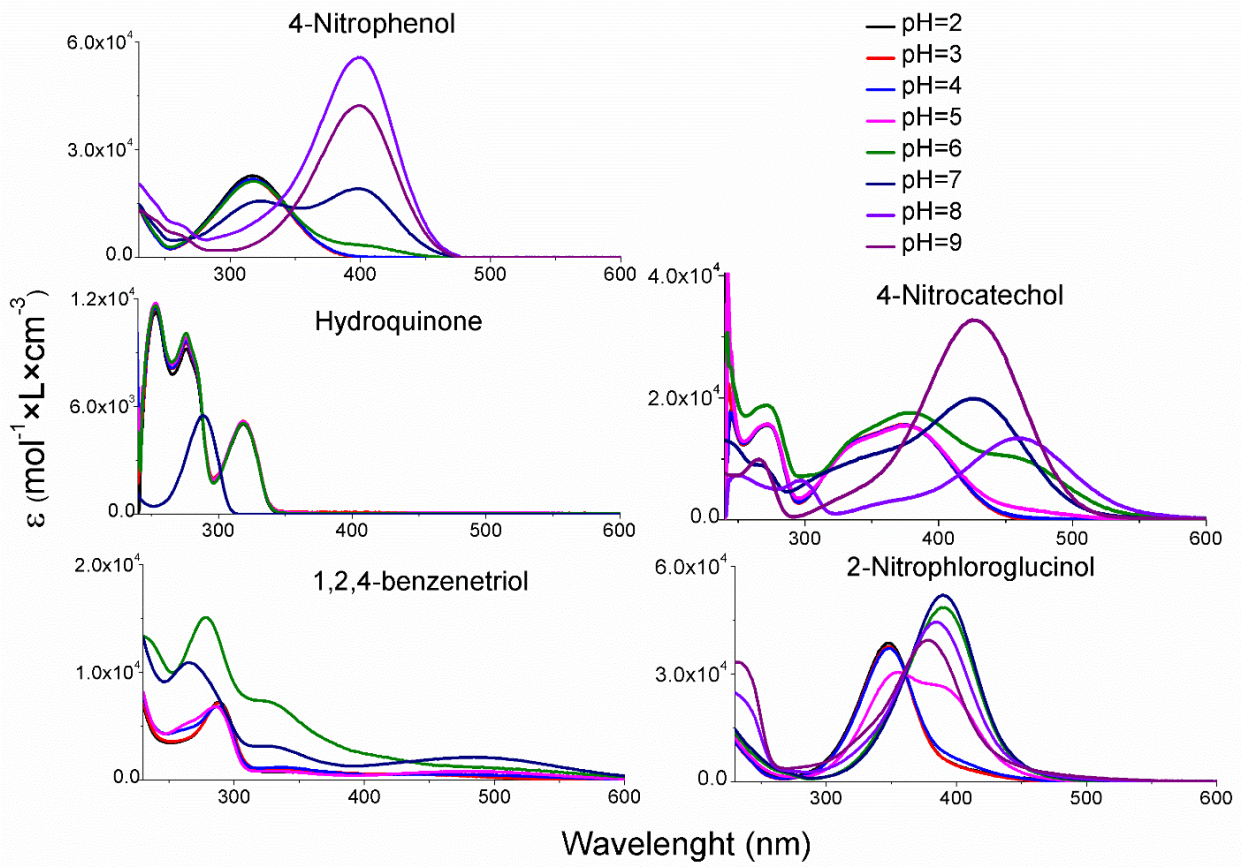

Figure S5: pH and wavelength-dependent UV-Vis absorption cross sections measured for 4-nitrophenol, hydroquinone, 4-nitrocatechol, 1,2,4-trihydroxybeneze and 2-nitrophloroglucinol in water.

Section S6. Control experiments

Control experiments listed in Table S2 were carried out using pure 4-nitrophenol or a mixture of compounds listed in Table S1. Due to large number of control experiments, the results obtained are summarized in Table S2, for clarity. The objective of the experiments listed was to evaluate whether or not any other processes, in addition to the reaction with the OH, contributed to the formation or disappearance of phenols under the investigation.

Table S2. Experimental conditions and results of the control experiments.

Compound name	**Reaction conditions**			**Results**
	pH	*UV*	H_2O_2	
4-nitrophenol, 4-Nitrocatechol, 2-Nitrophloroglucinol	2 (HCl or $HClO_4$) and 9 (Na_2HPO_4)	Yes	No	N/R
		No	Yes	
		No		
Hydroquinone, 1,2,4-Trihydroxybenzene	2 (HCl or $HClO_4$)	Yes	No	N/R
		No	Yes	
		No		
	7, 8, 9 (Na_2HPO_4)	Yes	No	Decomposition at pH>7
		No	Yes	
		No		

As listed in Table S2, none of the phenols under investigation underwent direct photolysis or "dark" reactions with H_2O_2, within the time-scale of the experiment. Moreover, stability of hydroquinone and 1,2,4-trihydroxybenzene depend on pH of the solution; these compounds either decomposed or underwent different "dark" reactions under basic pH conditions (Randolph et al., 2018). Concentration of 1,2,4-trihydroxybenzene decreased rapidly at pH>7, which is consistent with the previously published data (Liu et al., 2010).

Moreover, due to relatively fast and irreversible hydrolysis of hydroquinone and 1,2,4-trihydroxybenzene the pH-dependent ε values for these compounds were measured at pH<7. No derivatization artifacts (e.g. phenols that were not present in the standard solutions) were detected in any of the control experiments, thereby unambiguously confirming that 4-nitroresorcinol and 4-nitropyrogallol were produced from the reaction of OH with 4-nitrophenol, as it is presented in section 3.1.

2-Nitrophloroglucinol was stable in basic solution, as opposed to its structural isomers that were tentatively identified in the reaction mixture: 4-nitropyrogallol and 5-nitropyrogallol. Due to the lack of standards, the stability of these two products in basic solution was investigated indirectly, as described in section S7.

Section S7. Oxidation of 4-nitrocatechol via OH under acidic and basic conditions

A separate set of experiments was carried out with 4-nitrocatechol as a precursor; the experimental conditions and GC/MS analysis procedure were the same as in the experiments with 4-nitrophenol. The GC/MS chromatograms obtained are presented in Fig. S6 and S7.

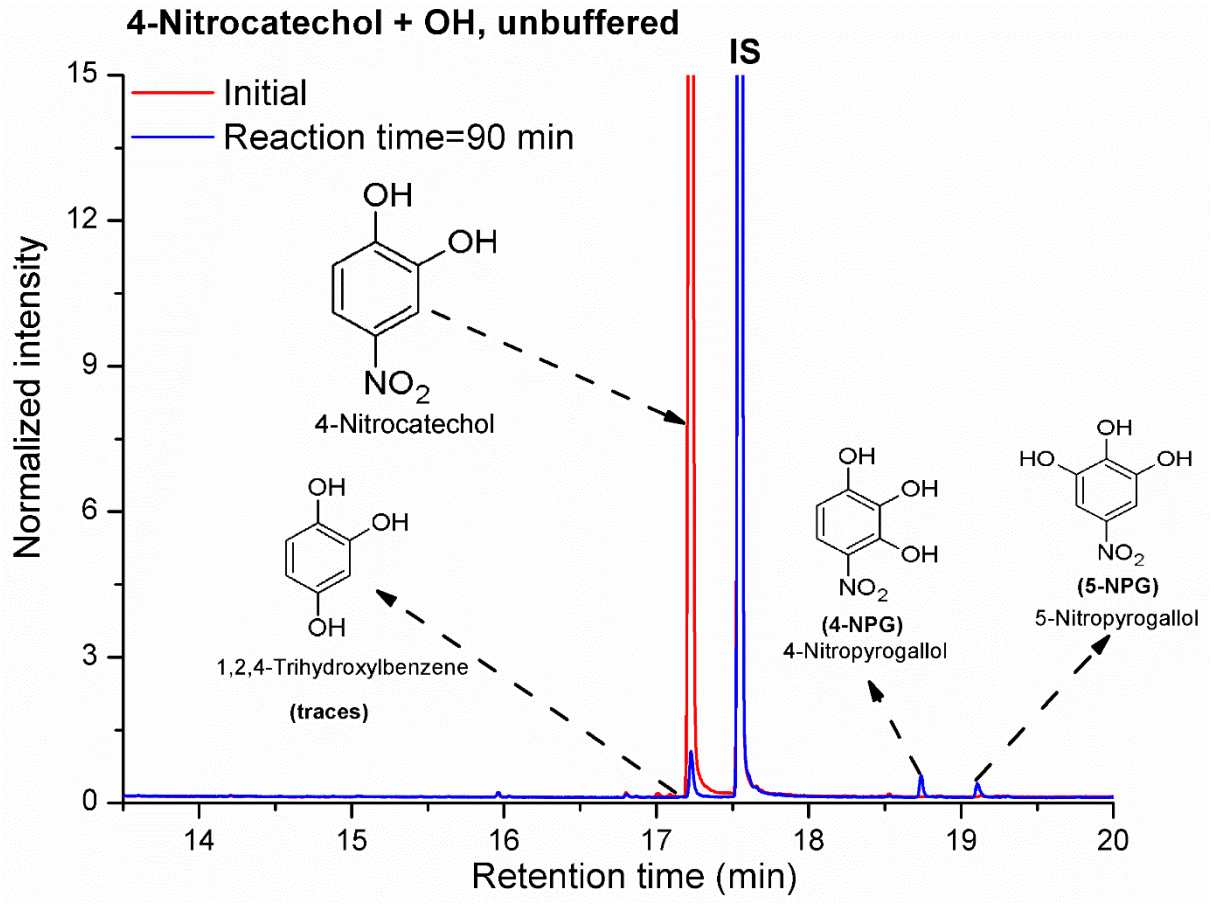

Figure S6: Chromatograms illustrating the formation of phenolic products from OH+4-nitrocatechol oxidation in pure DI water.

As presented in Fig. S6, the experimental data acquired unambiguously confirmed that 4-nitropyrogallol and 5-nitropyrogallol were formed following OH reaction with 4-nitrocatechol. Moreover, formation of 1,2,4-trihydroxybenzene was not observed; only a trace amount of this product detected in the reaction mixture. Analogously to the reaction of OH+4-NC, the pH of the reaction solution quickly decreased from the initial 6.4 to 3.2 within the first few minutes.

To check if 4-nitropyrogallol and 5-nitropyrogallol are stable at pH=9, oxidation of 4-nitrocatechol was carried out in basic solution – results are presented in Fig. S7.

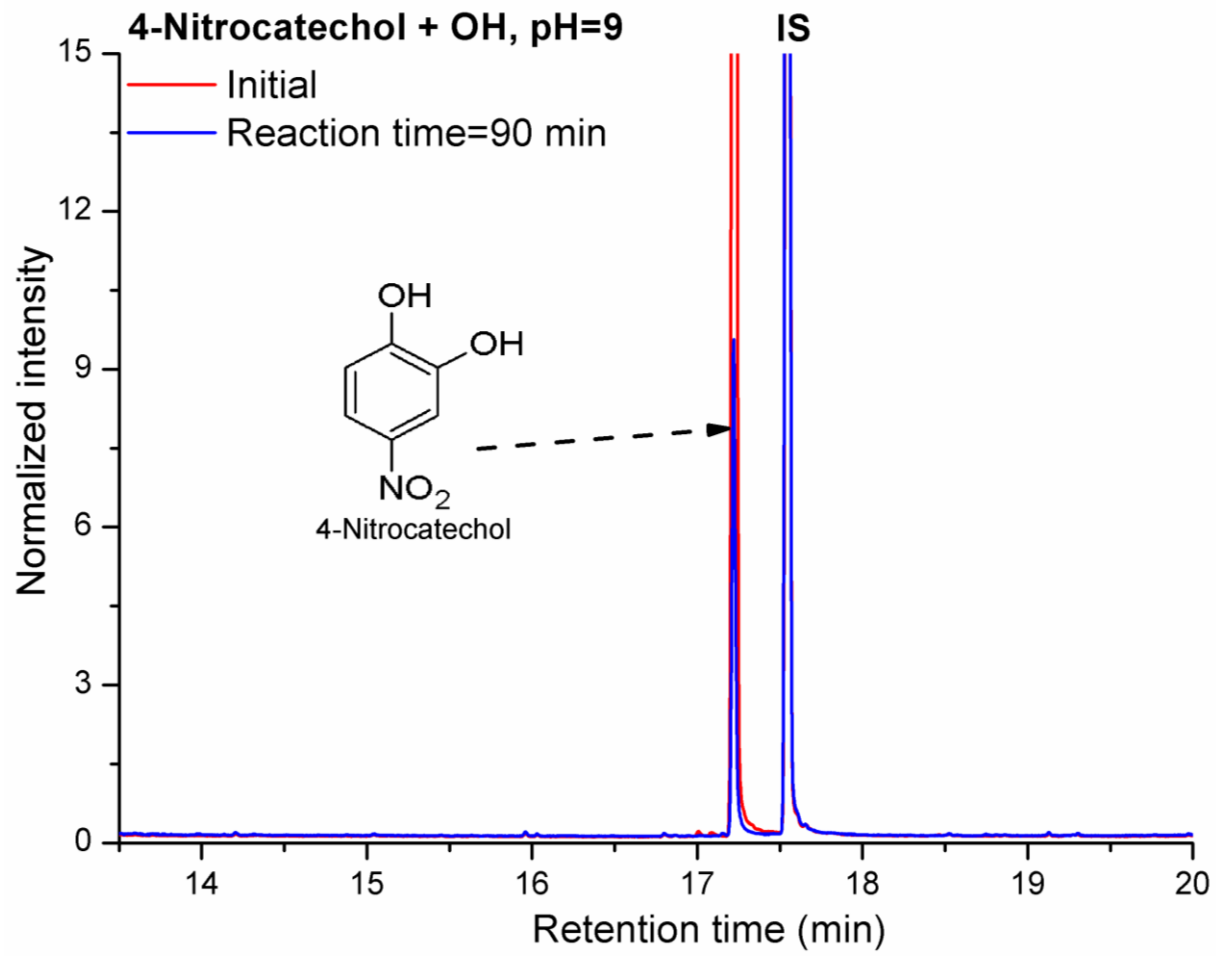

Figure S7: Chromatograms illustrating the formation of phenolic products from OH+4-nitrocatechol oxidation at pH=9

As presented in Fig. S7, the experimental data acquired confirmed that 4-nitropyrogallol and 5-nitropyrogallol were unstable at pH=9, because chromatographic peaks corresponding to these products were not observed.

Section S8. Evolution of light absorptivity of the reaction solution during reaction with OH

UV-Vis spectra, illustrating the evolution of the UV-Vis absorbance of the reaction solution and formation of the light-absorbing products are presented in Fig. S8.

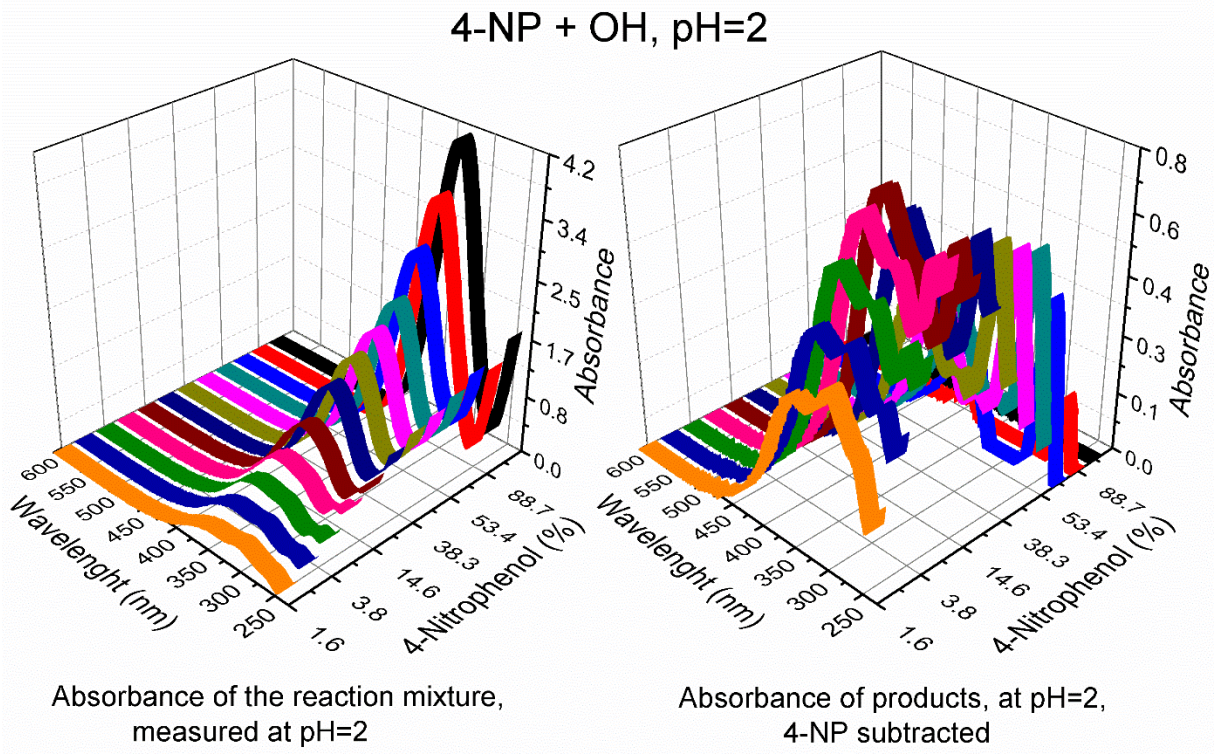

Figure S8: Evolution of the UV-Vis absorbance of the reaction mixture between 230 and 600 nm, reaction was carried out at pH=2 and the absorbance was measured at pH=2.

As presented in Fig. S8, the absorbance of the reaction mixture shows a steady decrease following the oxidation of 4-nitrophenol via OH. The absorbance of products was calculated by subtracting the absorbance of 4-nitrophenol from the measured absorbance of the reaction mixture using eq. SI

$$A_{products}(nm) = A_{r.mix}(nm) - A_{4-NP}(nm) \quad (SI)$$

The pH-dependent absorbance of 4-nitrophenol was calculated with eq. SII using the [4-nitrophenol] measured with GC/MS and pH as well as wavelength-dependent molar absorptivity of 4-nitrophenol (ε ; base-e; $mol^{-1} \times L \times cm^{-3}$):

$$A_{4-NP}(nm) = \frac{[4-NP] \times \varepsilon}{Ln(10)} \quad (SII)$$

As presented in Fig. S8, reaction of OH with 4-nitrophenol was generating light-absorbing products. For this reason, the bleaching 4-NP by OH is prolonged - Fig. S9.

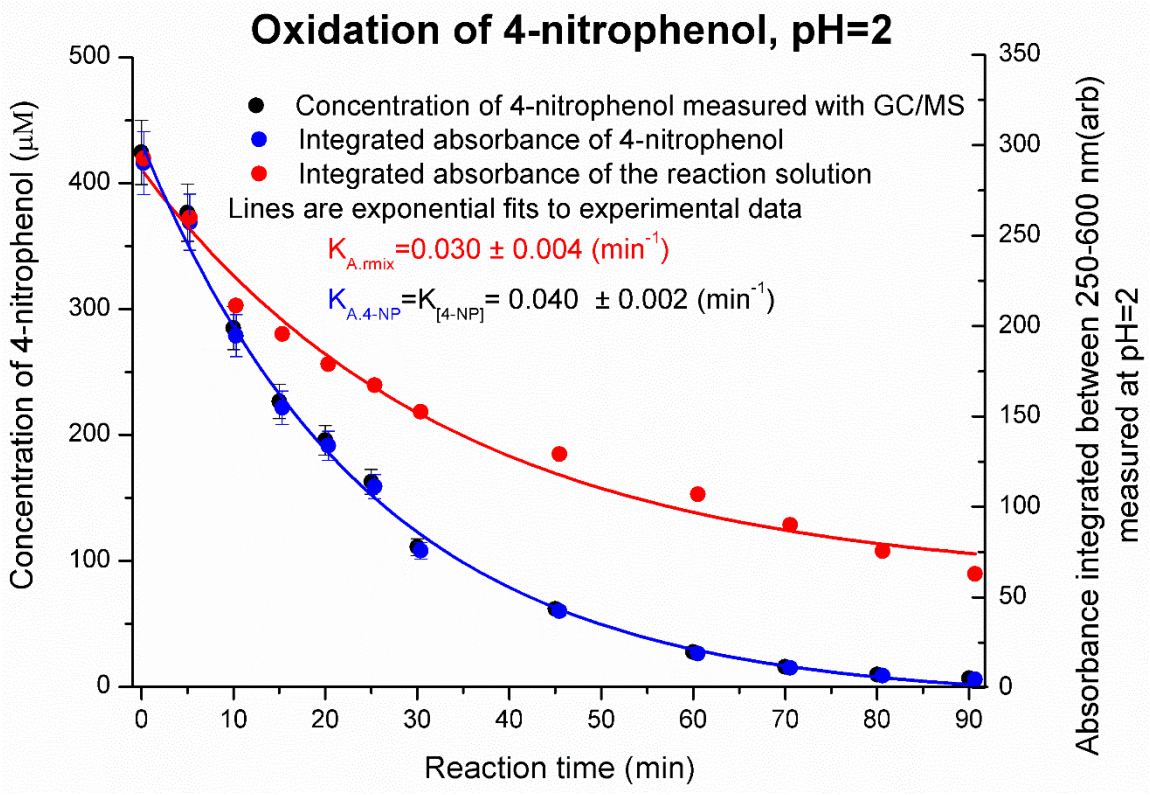

Figure S9: Prolonged bleaching of the chromophores in the 4-nitrophenol solution due to formation of light-absorbing by-products at pH=2.

As presented in Fig. S9, the disappearance of the integrated absorbance of reaction solution was slower than the disappearance of the integrated absorbance of 4-nitrophenol due to formation of light-absorbing products. To estimate the atmospheric lifetimes of the chromophores with a significant light absorptivity between 250 and 600 nm, the empirical $k_{bleaching}$ rate coefficients were calculated with eq. II. The first order-disappearance rates of integrated absorbance ($K_{A.rmix}$ and $K_{A.4\text{-}NP}$) were obtained via exponential fit to the experimental data shown in Fig. S9. The empirical $k_{bleaching}$ rate coefficients were derived with eq. II using the data acquired are listed in Table S3 and were used to estimate the atmospheric lifetimes of 4-NP BrC, as described in more detail in section S11.

To quantitatively evaluate the formation light-absorbing products under a given reaction conditions, the K_{abs} factor was introduced (eq. I). K_{abs} is used to describe the dependence between the normalized concentration of 4-nitrophenol and the $(\int_{250nm}^{600nm} A_{R.mix} d\lambda) / (\int_{250nm}^{600nm} A_{4-NP} d\lambda)$ ratio via eq. I.- Fig. S10.

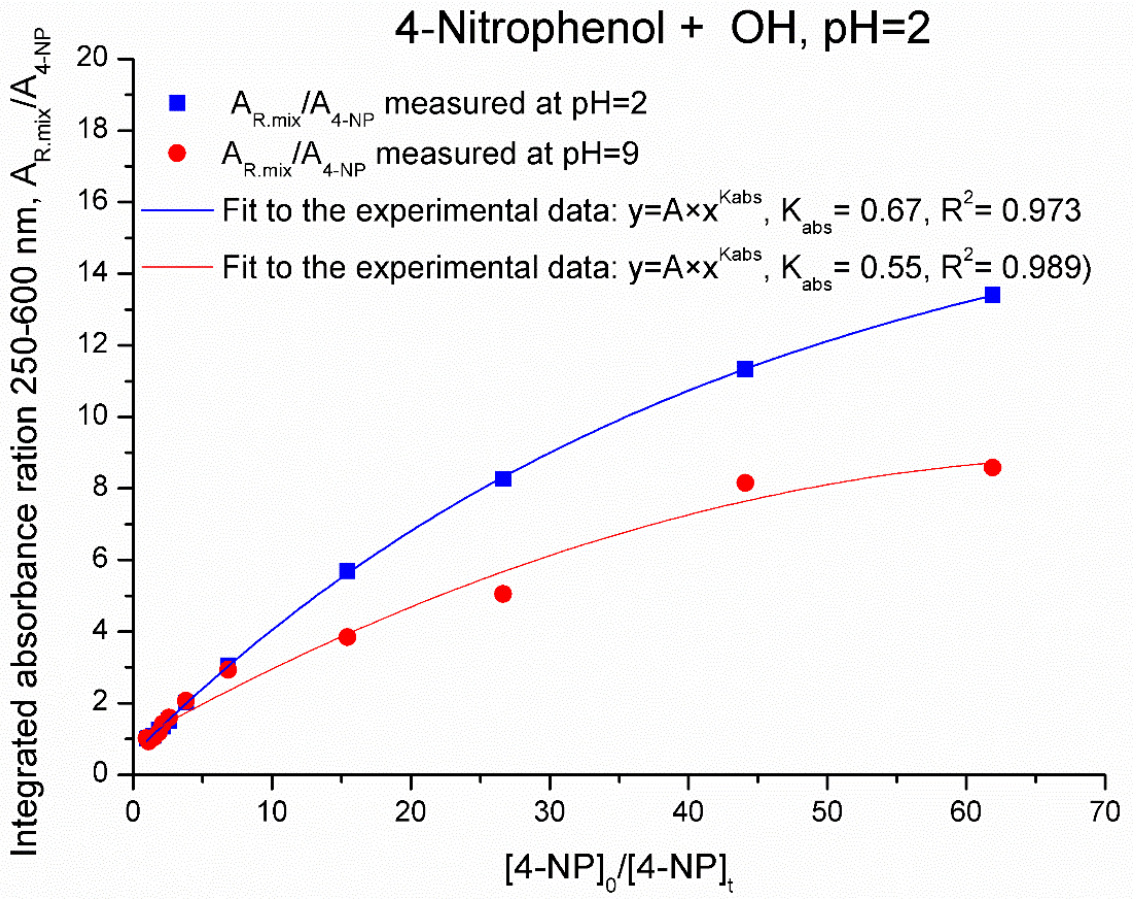

Figure S10:Sample data illustrating the derivation of Kabs factors via eq. I.

As presented in Fig. S10, lower value of K_{abs} corresponds to decreased ability of the reaction (1) to generate the light-absorbing products that essentially prolong the lifetime of BrC chromophores in the solution of 4-NP, under a given reaction conditions (pH). In other words, the absorptivity of the reaction mixture corresponding to the reaction products is increasing more slowly under a given conditions. K_{abs} factors were obtained for the reactions carried out in acidic and basic solutions. Consequently, for the experiments carried out at pH=2 and pH=9, eight K_{abs} factors were obtained because the absorptivity of the reaction solution was measured between pH=2 and 9 using intervals of 1 pH unit.

The K_{abs} derived where subsequently were plotted against the pH at which the absorbance was measured for the reaction carried out under acidic and basic pH - results are presented in Fig. S11.

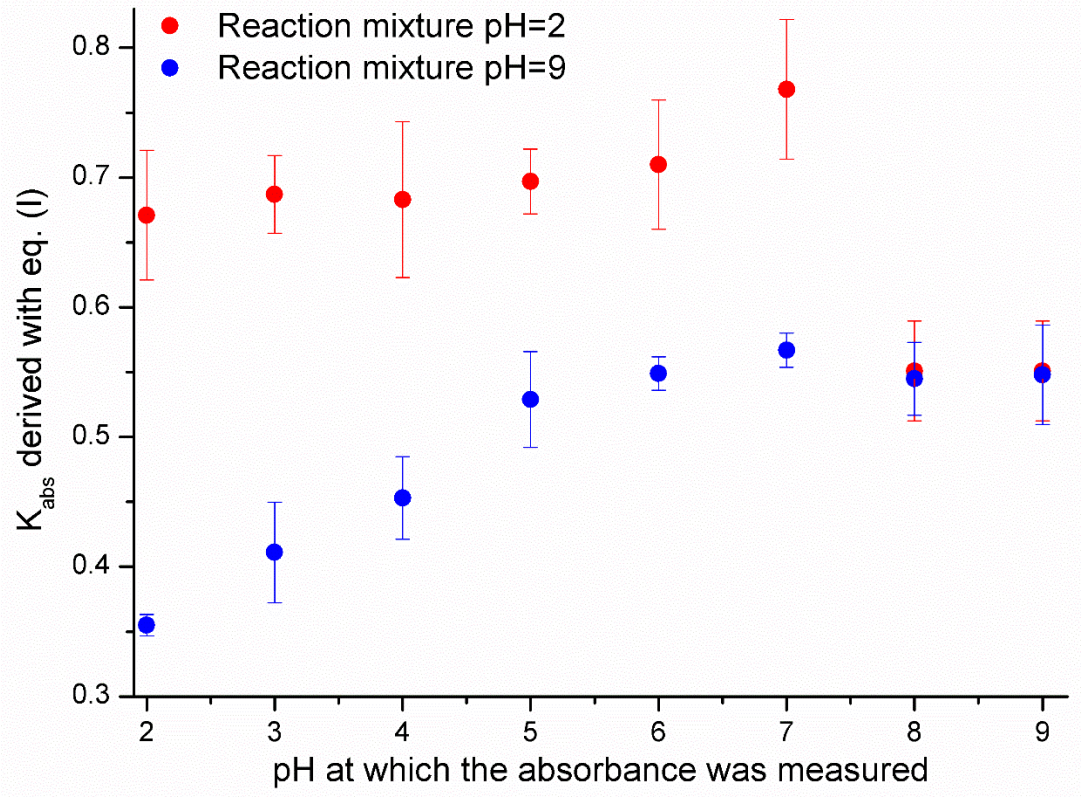

Figure S11: Ability of 4-nitrophenol to generate products characterized by a significant absorbance between 250 and 600 nm. Uncertainties are standard errors from the regression analysis.

As presented in Fig. S11, light-absorbing products was significantly clearly underwent irreversible reactions at pH=8 and 9. Moreover, absorbance of the products of 4-nitrophenolate reaction with OH (reaction solution pH=9) increased between pH=2 and 5 (Fig. 3), which cannot be explained by the changes in the absorbance of 4-NC which is constant in this pH range (Fig. S5). The observed increase in the light-absorptivity of the reaction solution (pH=9) between pH=2 and 9 can be due to pH-dependence of the absorbance of substituted carboxylic acids (aromatic ring-opening products) (Hems and Abbatt, 2018; Kavitha and Palanivelu, 2005; Zhang et al., 2003; Oturan et al., 2000) with pKa values likely falling between 3 and 6 (Rapf et al., 2017). Absorptivity of the products generated at pH=2 decrease sharply when the pH of the solution before the UV-Vis measurement was adjusted to 8 and 9. This is consistent with the "dark" decomposition of light-absorbing phenols (Sect. 3.1).

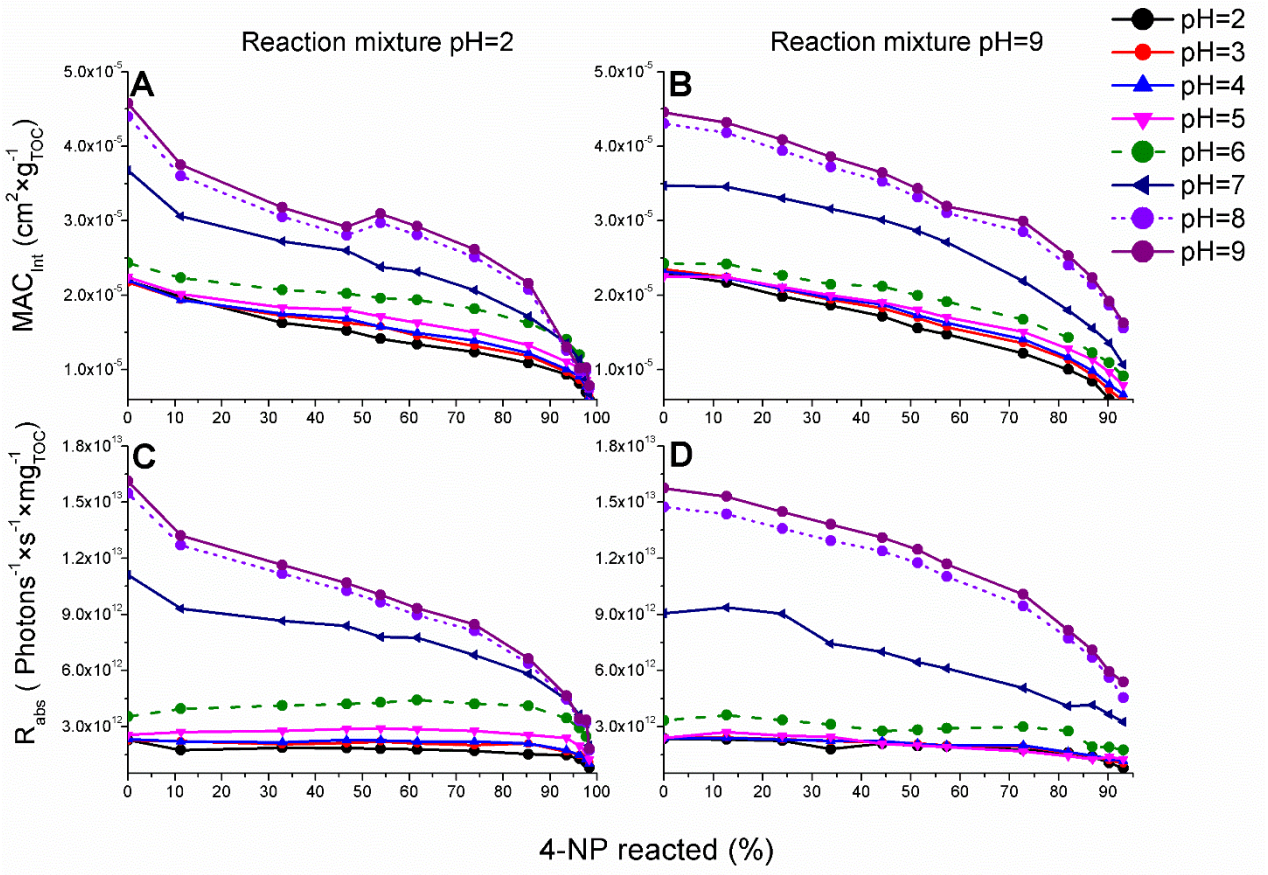

Figure S12: The pH dependent organic carbon-based mass absorption coefficients (MACint) derived using the integrated absorbance peaks of the reaction mixture measured for the reaction of 4-NP(A) and 4-nitrophenolate (B) and the corresponding TOC-normalized rates of sunlight absorption (Rabs) for of 4-NP (C) and 4-nitrophenolate (D).

Section S9. Air-water partitioning of 4-nitrophenol

The partitioning of 4-nitrophenol between aqueous and gaseous phase as a function of LWC of atmospheric particles (Herrmann et al., 2015) presented in Fig. S13 was estimated based on the Henry's constant – the average experimentally measured value is 5×104 (M×atm-1) (Sander, 2015).

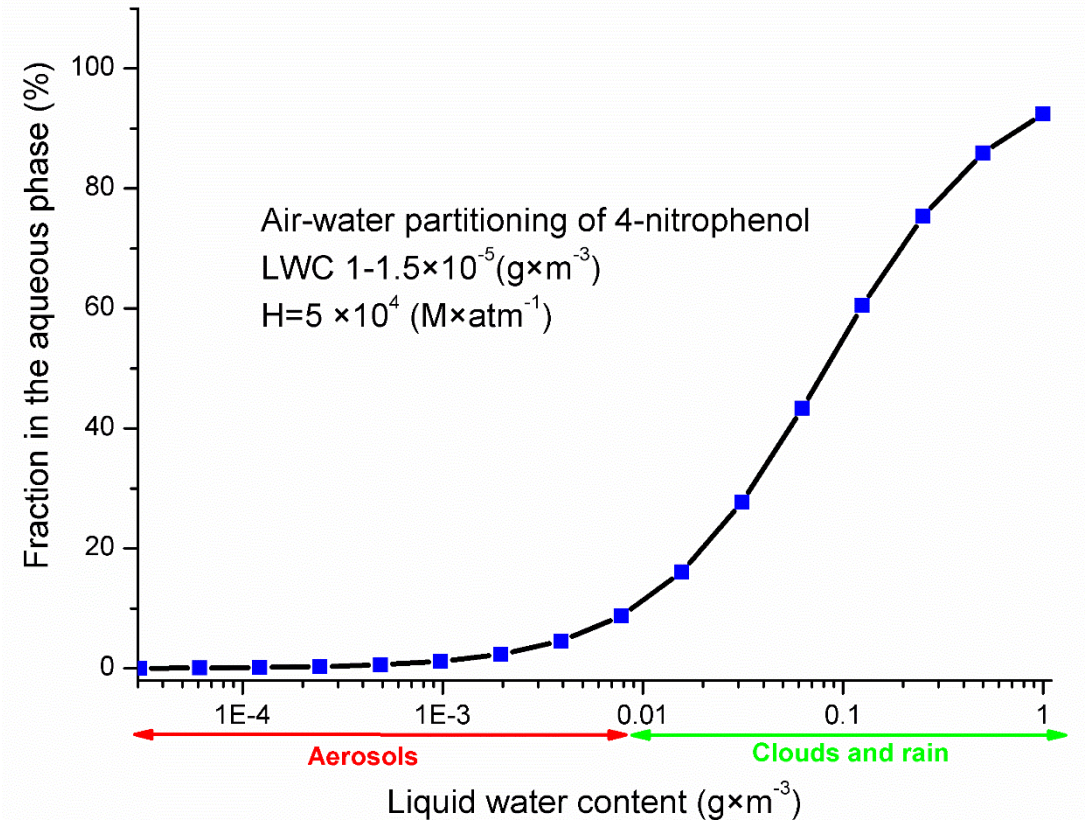

Figure S13: Partitioning of 4-NP based on the Henry's law equilibrium as a function of liquid water content.

Section S10. Atmospheric lifetimes and processing of 4-nitrophenol brown carbon

Atmospheric lifetimes for bleaching of 4-NP due to reaction with OH were calculated with eq. SIII.

$$\tau_{OH}(h) = \left(k_{bleaching} \times [OH]\right)^{-1} \times 3600^{-1} \quad (SIII)$$

In eq. SIII, $k_{bleaching}$ are the empirical rate coefficients,($M^{-1}s^{-1}$) for the bleaching of the aqueous solution of 4-nitrophenol/4-nitrophenolate by OH (Biswal et al., 2013) calculated using eq. II. [OH] is aqueous concentration of OH, in cloud water (Herrmann et al., 2010).

Atmospheric lifetimes for bleaching of 4-NP due to direct photolysis were calculated with eq. SIV.

$$\tau_{photolysis}(h) = \left(\int_{250nm}^{600nm} \phi \times \varepsilon_\lambda \times I_\lambda \times 1000 \times N_A^{-1}\right)^{-1} \times 3600^{-1} \quad (SIV)$$

In eq. SVI, ϕ is the quantum yield (molecules ×photon^{-1}), ε is a wavelength and pH-dependent base-e absorption cross section measured int his work for 4-NP (pH=2) or 4-nitrophenolate (pH>8) - see appendix 1 and Fig. S5 (mol^{-1} × L × cm^{-1}), I_λ is a the actinic flux (photons× s^{-1}× cm^{-2}×nm^{-1}) estimated with TUV calculator (Ncar, 2016) for zenith angles 0-50° (see Fig. S14) and N_A is Avogadro constant.

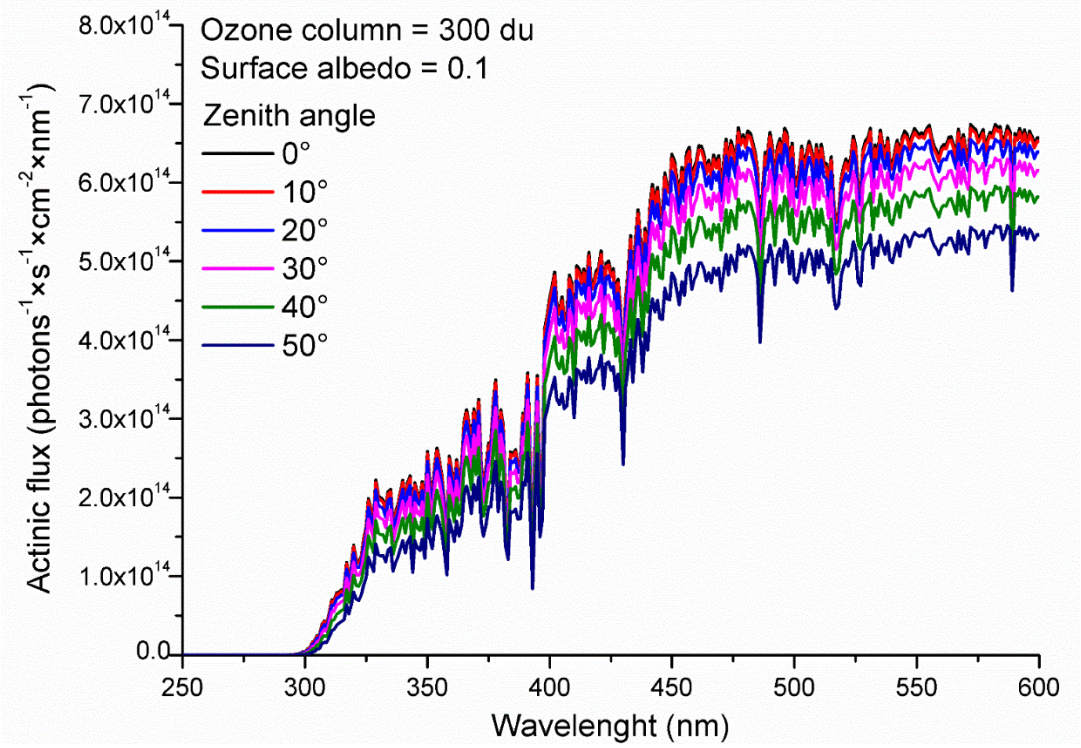

Figure S14: Actinic fluxes estimated with TUV calculator used to derive the Rabs values shown in Fig. 3 and photolysis lifetimes shown in Fig. 4. in the main text .

The data used to estimate the atmospheric lifetimes of 4-NP-derived atmospheric BrC is listed in Table S3.

Table S3. pH-dependent bimolecular rate coefficients, empirical bleaching rate coefficients and the effective quantum yields of photolysis used to estimate the lifetimes of 4-nitrophenols and the corresponding BrC

Reaction with OH						
Reactive species	**$K_{A.4\text{-}NP}$ (min^{-1})**	**$K_{A.rmix}$ (min^{-1})**	**$k_{OH} \times 10^{-9}$ ($M^{-1}s^{-1}$)**	**Reference**	**$k_{bleaching} \times 10^{-9}$ ($M^{-1}s^{-1}$) (this work)**	**Lifetimes of BrC relative to the lifetimes of 4-NP**
4-Nitrophenol (pH<3)	**0.047**	**0.016**	**6.2**	**(Biswal et al., 2013)**	**1.6**	**3**
			4.1	**(García Einschlag et al., 2003)**		
			3.8			
			4.7	**Average literature value**		
4-Nitrophenolate (pH>9)	**0.029**	**0.019**	**8.7**	**(Biswal et al., 2013)**	**6.0**	**1.5**
Photolysis						
Reactive species	**ϕ (molecules $\times$photon^{-1}) $\times$ 10^6**				**Reference**	
4-Nitrophenol (pH<3)	**110.0[a]**				**(Lemaire et al., 1985; Braman et al., 2020)**	
4-Nitrophenolate (pH>9)	**5.5**				**(Lemaire et al., 1985)**	

[a]This value measured in a presence of photorecalcitrant α-pinene SOA which acted as a scavenger of secondary OH formed following photolysis of HONO formed following photolysis of 4-NP [18] and it is practically the same as the average ϕ value previously derived via photometric measurement [19].

The empirical $k_{bleaching}$ rate coefficients were derived via eq. II to estimate the lifetimes of 4-NP and BrC associated with it as a function of cloud-water OH concentration (Bianco et al., 2020). Moreover, the literature ϕ values were used to estimate the lifetimes of 4-NP and BrC associated with it, results are presented in Fig. 4 in the main text

Section S11. Mineralization and formation of volatile products

Mineralization of 4-NP was investigated by carrying out TOC measurements (Sect. 2.5) – the results are presented in Fig. S15.

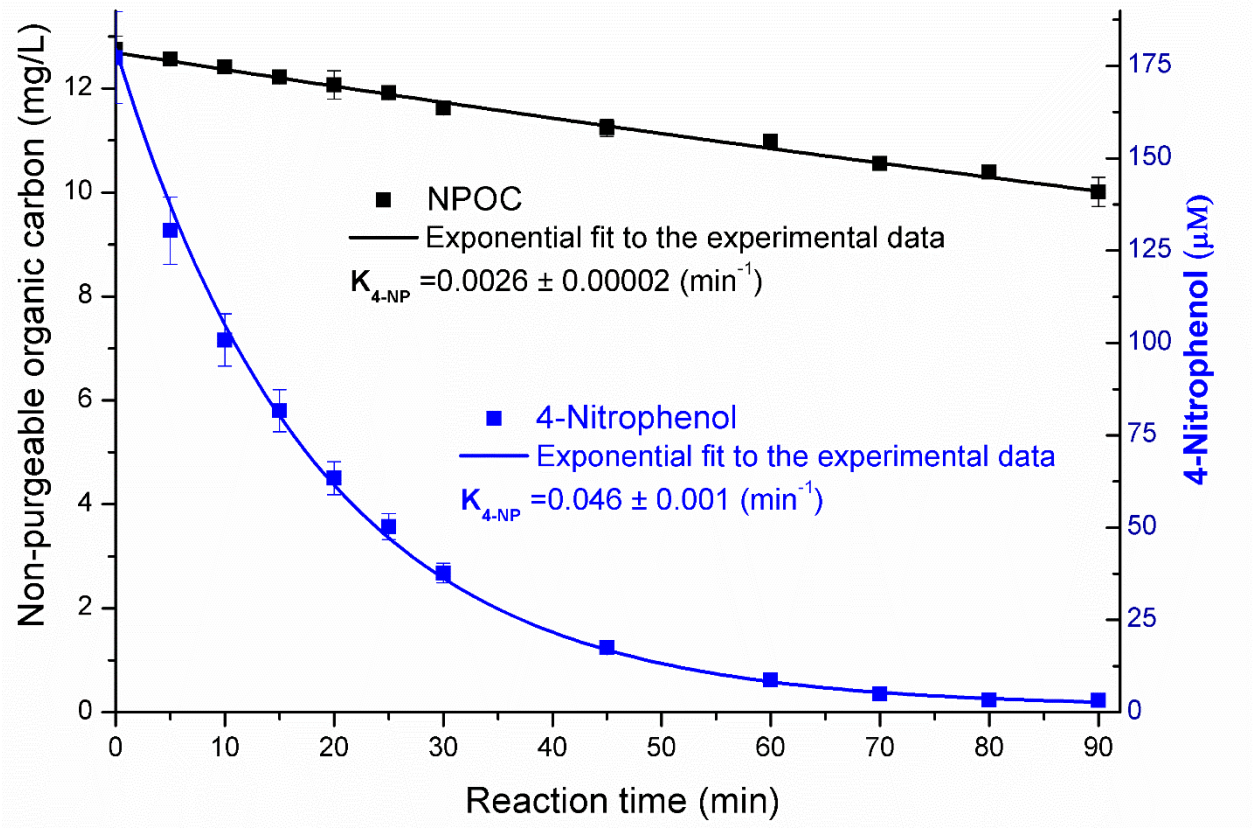

Figure S15: Concentrations of 4-NP and non-purgeable organic carbon during the reaction of pure DI water. Uncertainties for the first-order decay rates (K, min-1) are standard errors from regression analysis.

Very similar data from the TOC measurements was obtained when the reaction was carried out at pH=2 and 9. For this reason, only the data for the unbuffered solution is presented in Fig. S15. The of TOC measurements confirmed that after 4-NP was completely consumed, 85% of initial organic carbon remains in the aqueous phase, similar results were also reported in the previously published studies (Liu et al., 2010; Zhang et al., 2003). This indicates that, following the reaction with OH, 4-NP is primarily converted into ring-opening products that are characterized by the lower UV-Vis absorptivity than the precursor and phenolic products, leading to the overall decrease in the absorption the reaction solution (Fig. 3). These results are in a good agreement with the overall decrease in the absorptivity of the reaction solution combined with the fact that 4-NP effectively exhibits a significant resistance to chemical bleaching by OH.

References

Bianco, A., Passananti, M., Brigante, M., and Mailhot, G.: Photochemistry of the Cloud Aqueous Phase: A Review, Molecules, 25, 10.3390/molecules25020423, 2020.

Biswal, J., Paul, J., Naik, D. B., Sarkar, S. K., and Sabharwal, S.: Radiolytic degradation of 4-nitrophenol in aqueous solutions: Pulse and steady state radiolysis study, Radiation Physics and Chemistry, 85, 161-166, https://doi.org/10.1016/j.radphyschem.2013.01.003, 2013.

Braman, T., Dolvin, L., Thrasher, C., Yu, H., Walhout, E. Q., and O'Brien, R. E.: Fresh versus Photo-recalcitrant Secondary Organic Aerosol: Effects of Organic Mixtures on Aqueous Photodegradation of 4-Nitrophenol, Environmental Science & Technology Letters, 7, 248-253, 10.1021/acs.estlett.0c00177, 2020.

García Einschlag, F. S., Carlos, L., and Capparelli, A. L.: Competition kinetics using the UV/H2O2 process: a structure reactivity correlation for the rate constants of hydroxyl radicals toward nitroaromatic compounds, Chemosphere, 53, 1-7, https://doi.org/10.1016/S0045-6535(03)00388-6, 2003.

Hems, R. F. and Abbatt, J. P. D.: Aqueous Phase Photo-oxidation of Brown Carbon Nitrophenols: Reaction Kinetics, Mechanism, and Evolution of Light Absorption, ACS Earth and Space Chemistry, 2, 225-234, 10.1021/acsearthspacechem.7b00123, 2018.

Herrmann, H., Hoffmann, D., Schaefer, T., Bräuer, P., and Tilgner, A.: Tropospheric Aqueous-Phase Free-Radical Chemistry: Radical Sources, Spectra, Reaction Kinetics and Prediction Tools, ChemPhysChem, 11, 3796-3822, https://doi.org/10.1002/cphc.201000533, 2010.

Herrmann, H., Schaefer, T., Tilgner, A., Styler, S. A., Weller, C., Teich, M., and Otto, T.: Tropospheric Aqueous-Phase Chemistry: Kinetics, Mechanisms, and Its Coupling to a Changing Gas Phase, Chem. Rev., 115, 4259-4334, 10.1021/cr500447k, 2015.

Kavitha, V. and Palanivelu, K.: Degradation of nitrophenols by Fenton and photo-Fenton processes, Journal of Photochemistry and Photobiology A: Chemistry, 170, 83-95, https://doi.org/10.1016/j.jphotochem.2004.08.003, 2005.

Lemaire, J., Guth, J. A., Klais, O., Leahey, J., Merz, W., Philp, J., Wilmes, R., and Wolff, C. J. M.: Ring test of a method for assessing the phototransformation of chemicals in water, Chemosphere, 14, 53-77, https://doi.org/10.1016/0045-6535(85)90041-4, 1985.

Liu, Y., Wang, D., Sun, B., and Zhu, X.: Aqueous 4-nitrophenol decomposition and hydrogen peroxide formation induced by contact glow discharge electrolysis, Journal of Hazardous Materials, 181, 1010-1015, https://doi.org/10.1016/j.jhazmat.2010.05.115, 2010.

TUV calculator: https://www.acom.ucar.edu/Models/TUV/Interactive_TUV/, last

Oturan, M. A., Peiroten, J., Chartrin, P., and Acher, A. J.: Complete Destruction of p-Nitrophenol in Aqueous Medium by Electro-Fenton Method, Environmental Science & Technology, 34, 3474-3479, 10.1021/es990901b, 2000.

Randolph, C., Lahive, C. W., Sami, S., Havenith, R. W. A., Heeres, H. J., and Deuss, P. J.: Biobased Chemicals: 1,2,4-Trihydroxybenzene, Selective Deuteration and Dimerization to Bifunctional Aromatic Compounds, Organic Process Research & Development, 22, 1663-1671, 10.1021/acs.oprd.8b00303, 2018.

Rapf, R. J., Dooley, M. R., Kappes, K., Perkins, R. J., and Vaida, V.: pH Dependence of the Aqueous Photochemistry of α-Keto Acids, The Journal of Physical Chemistry A, 121, 8368-8379, 10.1021/acs.jpca.7b08192, 2017.

Sander, R.: Compilation of Henry's law constants (version 4.0) for water as solvent, Atmos. Chem. Phys., 15, 4399-4981, 10.5194/acp-15-4399-2015, 2015.

Tan, Y., Perri, M. J., Seitzinger, S. P., and Turpin, B. J.: Effects of Precursor Concentration and Acidic Sulfate in Aqueous Glyoxal−OH Radical Oxidation and Implications for Secondary Organic Aerosol, Environmental Science & Technology, 43, 8105-8112, 10.1021/es901742f, 2009.

Vione, D., Maurino, V., Minero, C., Duncianu, M., Olariu, R.-I., Arsene, C., Sarakha, M., and Mailhot, G.: Assessing the transformation kinetics of 2- and 4-nitrophenol in the atmospheric aqueous phase. Implications for the distribution of both nitroisomers in the atmosphere, Atmospheric Environment, 43, 2321-2327, https://doi.org/10.1016/j.atmosenv.2009.01.025, 2009.

Witkowski, B., Al-sharafi, M., and Gierczak, T.: Kinetics and products of the aqueous-phase oxidation of β-caryophyllonic acid by hydroxyl radicals, Atmospheric Environment, 213, 231-238, https://doi.org/10.1016/j.atmosenv.2019.06.016, 2019.

Zhang, W., Xiao, X., An, T., Song, Z., Fu, J., Sheng, G., and Cui, M.: Kinetics, degradation pathway and reaction mechanism of advanced oxidation of 4-nitrophenol in water by a UV/H2O2 process, Journal of Chemical Technology & Biotechnology, 78, 788-794, https://doi.org/10.1002/jctb.864, 2003.

Zhao, R., Lee, A. K. Y., Huang, L., Li, X., Yang, F., and Abbatt, J. P. D.: Photochemical processing of aqueous atmospheric brown carbon, Atmos. Chem. Phys., 15, 6087-6100, 10.5194/acp-15-6087-2015, 2015.